

## Research Article

### Research on Port Food Transportation Port Food Transportation Mooring Load Prediction through Theoretical Calculation Model with the Wavelet Analysis

<sup>1,2</sup>Zheng Jian, <sup>2</sup>Xiao Ying-Jie and <sup>2</sup>Zhang Hao

<sup>1</sup>College of Transport and Communications,

<sup>2</sup>Engineering Research Center of Simulation Technology, Ministry of Education, Shanghai Maritime University, Shanghai 201306, China

**Abstract:** In order to achieve the short-term and high-precision port food transportation port food transportation mooring load prediction, a new principle and method of ship's port food transportation port food transportation mooring load measurements based on indirect measurement is presented in this study and an algorithm is proposed through which predictions are made by comb the wavelet multi-scale decomposition and reconstruction method. Simulation results show that the combined algorithm has achieved short-term and high-precision port food transportation port food transportation mooring load prediction results, that it has excellent subdivision and self-learning abilities and that it can meet the accuracy requirement of the port food transportation port food transportation mooring load prediction in engineering.

**Keywords:** BP neural network, indirect measurement, mooring load, port food transportation

## INTRODUCTION

The short-term port food transportation port food transportation mooring load prediction and measurement, which is the core of port food transportation port food transportation mooring load monitoring and warning system, is an important component of the monitoring and warning of production and operation security in harbors (He *et al.*, 2002). Obtaining real-time port food transportation port food transportation mooring load data from the port food transportation port food transportation mooring load monitoring system may enable the mastery of the status of loads received by cables, but it is more difficult to determine the changes in port food transportation mooring load s in the future. Once such emergencies as a mooring cable breaks, there will be a lack of response time in which an emergency is disposed of, which will cause tremendous losses to the hydraulic construction of ships and piers (Liu *et al.*, 2010). Then the effective short-term port food transportation port food transportation mooring load prediction can improve the reliability of mooring safety warnings and win valuable time to dispose of hazardous situations of mooring to ensure the safety of the hydraulic construction of ships and piers (Dou *et al.*, 2009).

As port food transportation mooring load s are affected not only by environmental factors like winds, streams and waves but also by factors like the hull form

of ships, windage areas and draft sizes (Wu *et al.*, 2010). Therefore, being quite random and complex, they are non-stationary time series.

In this study, the theoretical model for the calculation on bollard surface stress under port food transportation port food transportation mooring load is built. The bollard surface stress is measured by means of strain electrical measuring method. The simultaneous equations of measurement value and theoretical calculation model are built. And the axial component and a radial component of port food transportation port food transportation mooring load are obtained and the port food transportation port food transportation mooring load is composed (Liang and He, 2011). Then, in connection with the feature that the short-term port food transportation port food transportation mooring load series is quite random and complex, the wavelet multi-scale decomposition method is used to decompose port food transportation port food transportation mooring load series into low-frequency approximation decomposition coefficients and layer high-frequency detail decomposition coefficients, to rebuild decomposition coefficients of each layer respectively into approximation components and multilayer detail components and to synthesize prediction results of each layer into desired prediction values. This provides an effective combined prediction method for the short-term port food transportation port food transportation mooring load prediction (Wang *et al.*, 2011).

**Corresponding Author:** Zheng Jian, College of Transport and Communications, Shanghai Maritime University, Shanghai 201306, China

This work is licensed under a Creative Commons Attribution 4.0 International License (URL: <http://creativecommons.org/licenses/by/4.0/>)

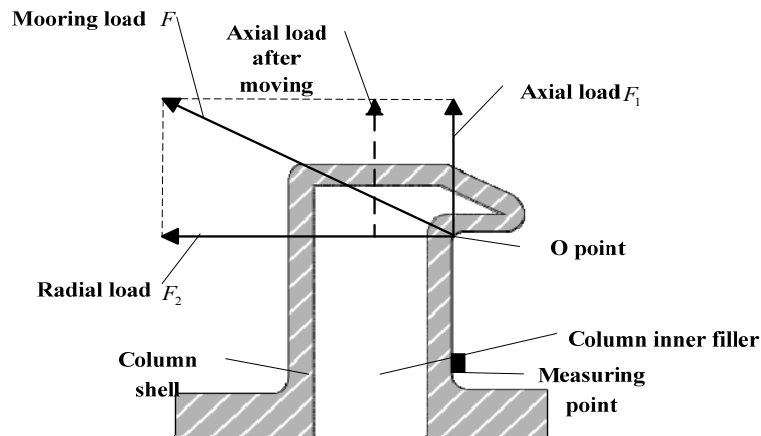


Fig. 1: Bollard structure and force analysis

## MATERIALS AND METHODS

**Theoretical calculation model of stress at measuring point on bollard surface:** Theoretical calculation model is built to measuring the port food transportation mooring load which is difficult to be measured directly. So theoretical calculation model can be used to indirect measure the port food transportation mooring load based on the bollard. The bollard body consists of column shell and column inner filler, of which the column shell is generally made of cast steel or cast iron and the column inner filler is made of concrete or asphalt concrete.

**Calculation of tensile stress:** Since the axial load line of bollard does not pass through the bollard axis, bollard section will generate deviation due to uneven axial load. To overcome this uneven force which moves the axial load to the axis horizontally, a force couple needs to be added and its torque is the torque of axial load  $F_1$  to the axis, namely  $M_z = F_1 \times R$ , where R is the radius of bollard cross-section. After translation, tensile stress generated by the axial load will distribute on the bollard cross-section evenly (Fig. 1).

When the bollard gives rise to axial tension caused by the axial load, linear strain of various vertical line segments will be same, so the tensile strain  $\varepsilon'$  caused by the axial load at each measuring point is same. According to the Hooke Theorem, axial load is as follows:

$$F_1 = \varepsilon'(E_1 A_1 + E_2 A_2) \quad (1)$$

where,

- $A_1$  = The cross-sectional area of column shell
- $A_2$  = The cross-sectional area of column inner filler
- $E_2$  = The elastic modulus of column inner filler

Then, the tensile stress caused by the axial force is:  $\sigma' = E_1 \varepsilon'$ ; according to formula (1),  $\varepsilon'$  can be expressed as  $\sigma' = E_1 F_1 / (E_1 A_1 + E_2 A_2)$ .

**Calculation of bending stress:** Radial load  $F_2$  causes bending deflection of bollard and only generates action of bending moment to neutral axis z on bollard cross-section. Since the bending rigidity of bollard is great, which generates small bending deflection, the additional bending moment caused by axial load is small, which can be negligible. Therefore, cross-sectional bending moment M on bollard is the sum of cross-sectional bending moment  $M_1$  on column shell and cross-sectional bending moment  $M_2$  on column inner filler, namely:

$$M = M_1 + M_2 = E_1 I_{z_1} / \rho + E_2 I_{z_2} / \rho \quad (2)$$

where,  $I_{z_1}$  is the inertia moment of neutral axis z of column shell cross-section,  $I_{z_2} = \pi ((2R)^4 - (2r)^4) / 64$ ;  $I_{z_2}$  is the inertia moment of neutral axis z of column inner filler cross-section,  $I_{z_2} = \pi (2r)^4 / 64$ ; r is the radius of column inner filler cross-section;  $\rho$  is radius of curvature of neutral layer.

$1/\rho = M / (E_1 I_{z_1} + E_2 I_{z_2})$  can be got according to formula (2); then, bending moment of column shell cross-section  $M_1 = E_1 I_{z_1} / \rho = E_1 I_{z_1} M / (E_1 I_{z_1} + E_2 I_{z_2})$ , where M is the sum of bending moment generated by radial load  $F_2$  and bending moment generated by translation of axial load, namely  $M = F_1 R + F_2 l$ ; l is the distance between the point of load and the measuring point cross-section of bollard cable.

Then, the bending stress at the measuring point is  $\sigma'' = M_1 y / I_{z_1}$ , where y is the distance between the measuring point and neutral axis.

In order to determine the distance between each measuring point and the neutral axis, arc length  $S_{A_1 B}$  and  $S_{A_2 B}$  from measuring point A1 and A2 to point B

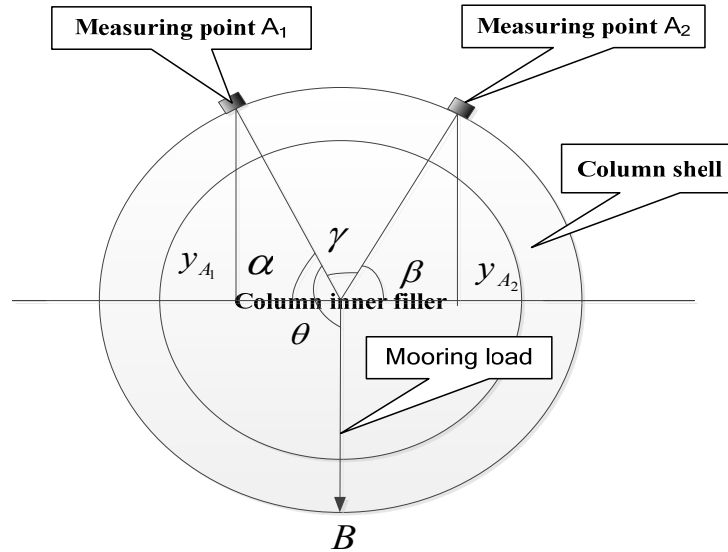


Fig. 2: The distance between each measuring point and the neutral axis

which is the intersection of the projection of cable load direction on bollard cross section and the cross section before measurement (ship may move back and forth in the case of mooring, resulting in minor change of the contact point of cable and bollard; however, such change is slow and the system is subject to measurement and design in a short time. Field surveyors can quickly measure the arc length again and modify the parameters in the measurement system when finding that the contact point changes significantly in the case of measurement. In the future, displacement sensors can be chosen to fuse to the system established in this text for real-time detection of the contact point of the cable and bollard if the development of cable load monitoring system is subject to the measurement for a long time), so the included angle between the line of measuring point and center of circle of the cross section and neutral axis  $z$  is  $\alpha = S_{A_1B}/R - \pi/2$  and  $\beta = S_{A_2B}/R - \pi/2$  (Fig. 2) and then, distance between the measuring point and the neutral axis is  $y_{A_1} = R \sin \alpha$  and  $y_{A_2} = R \sin \beta$ . As shown in Fig. 2.

Therefore, the bending stress at measuring point can be expressed as  $\sigma''_i = E_1(F_2l + F_1R) y_i / (E_1 I_{z_1} + E_2 I_{z_2})$ , where  $\sigma''_i$  is the bending stress at measuring point  $i$  and  $y_i$  is the distance between measuring point  $i$  and the neutral axis.

**Superposition of stress at measuring point:** After the tensile stress caused by axial load at measuring point and the bending stress caused by radial load are calculated respectively, stress  $\sigma_i$  at measuring point caused by the two kinds of load jointly can be obtained by using superposition principle, which is as follows:

$$\sigma_i = \sigma' + \sigma'' = E_1 \frac{F_1}{E_1 A_1 + E_2 A_2} + \frac{E_1(F_2l + F_1R)}{E_1 I_{z_1} + E_2 I_{z_2}} y_i \quad (3)$$

**The wavelet decomposition of port food transportation port food transportation mooring load series:**

The wavelet space decomposition is to decompose original frequency space into a series of high-frequency subspaces which reflect details and a low-frequency subspace which reflects an overview and to carry out analysis. The port food transportation port food transportation mooring load series is a set of time series, the basic steps of whose wavelet decomposition are as follows:

Let  $\psi(t)$  be a square integral function, i.e.,  $\psi(t) \in L^2(R)$ . If its Fourier transform meets the admissibility condition:

$$C_\psi = \int_R \frac{|\hat{\psi}(\omega)|^2}{|\omega|} d\omega < \infty \quad (4)$$

$\psi(t)$  is called a basic wavelet. After the basic wavelet is scaled and translated, a wavelet series can be obtained:

$$\psi_{a,b}(t) = \frac{1}{\sqrt{|a|}} \psi\left(\frac{t-b}{a}\right) \quad (5)$$

In the above formula,  $a$  is referred to as the scale factor,  $b$  is referred to as shift factor. The continuous wavelet transform of a square integral function  $f(t) \in L^2(R)$  is:

$$Wf(t) = \langle f, \psi_{a,b} \rangle = |a|^{-\frac{1}{2}} \int_R f(t) \psi^*\left(\frac{x-b}{a}\right) dt \quad (6)$$

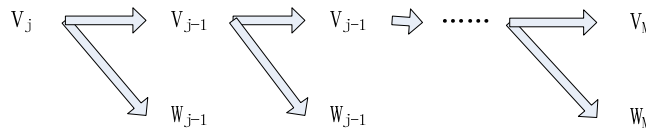


Fig. 3: The process of wavelet decomposition

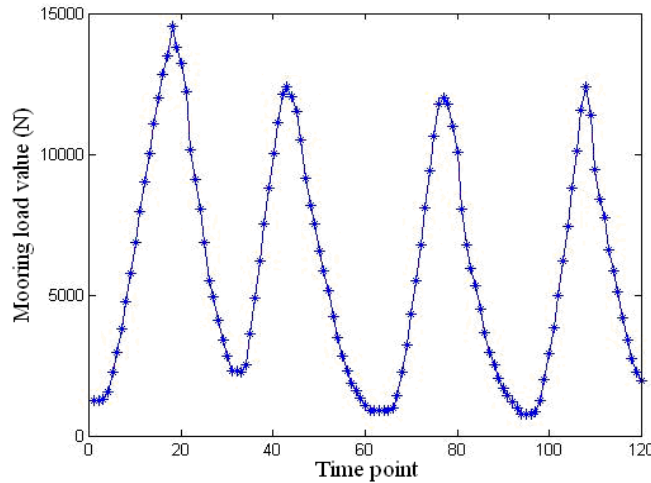


Fig. 4: The diagram of original port food transportation port food transportation mooring load series

In the above formula,  $\langle f, \psi_{a,b} \rangle$  the inner product of  $f(t)$  with  $\psi_{a,b}(t) \cdot \psi^*\left(\frac{x-b}{a}\right)$  is he conjugated function of  $\psi\left(\frac{x-b}{a}\right)$ .

As can be learnt by the Mallat algorithm of the wavelet series, the hierarchical decomposition of series  $f(t)$  can be expressed as:

$$f(t) = A_1 f + D_1 f = A_2 f + D_1 f + D_2 f = \dots = A_n f + D_1 f + \dots + D_n f \quad (7)$$

In the multi-resolution analysis conditions, according to formula (7), port food transportation port food transportation mooring load series can be decomposed into:

$$v(t) = a^N(k) + d^1(k) = a^2(k) + d^1(k) + d^2(k) = \dots = a^N(k) + \sum_{j=1}^N d^j(k) \quad (8)$$

Wherein  $a^N(k)$  is the decomposition coefficients of the low-frequency port food transportation port food transportation mooring load series of layer  $N$  ( $j = 1, 2, \dots, N$ ) is the decomposition coefficients of the high-frequency port food transportation port food transportation mooring load series of layer 1 to layer  $N$ . The decomposition process is shown as in Fig. 3.

According to the low-frequency coefficients of the  $N$ th layer and the high frequency coefficients of 1st to  $N$ th layer of wavelet decomposition, the wavelet

reconstruction of the port food transportation port food transportation mooring load components of each layer is carried out and a quite stable layer  $N$  approximation component  $V^N(t)$  and the high frequency detail component  $W^j(t+1)$  ( $j = 1, 2 \dots N$ ) of layer 1 to layer  $N$  can be obtained.

## RESULTS AND DISCUSSION

The original port food transportation port food transportation mooring load series collected by the port food transportation port food transportation mooring load monitoring system which is based on theoretical calculation model of stress at measuring point on bollard surface is modeled and predicted by using combined prediction algorithm proposed in this study. The 120 time series data collected through experiments (with a time interval of 30 sec) (Fig. 4) are verified through experiments by using the cable load monitoring system. 100 data is selected as initial samples to make predictions about the 20 data that follows.

**The multi-scale decomposition and reconstruction of port food transportation port food transportation mooring load series:** By using the Mallat tower algorithm, the Daubechies 3 wavelet is selected to decompose the original port food transportation port food transportation mooring load series into three layers of wavelets and coefficients of each layer which have undergone decomposition are reconstructed at different

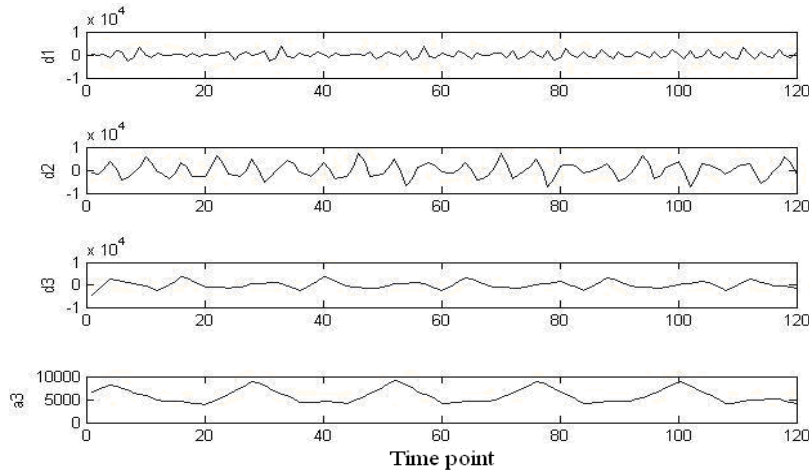


Fig. 5: The components of each layer after the wavelet decomposition and reconstruction by three layers

scales. The high-frequency component series layers 1 to 3 is denoted as  $d^1$ ,  $d^2$ ,  $d^3$  and the low frequency component series of layer 3 is denoted as  $a^3$  (Fig. 5).

### CONCLUSION

Due to the combined effects of quite a number of factors, port food transportation port food transportation mooring load measurement method which is based on theoretical calculation model of stress at measuring point on bollard surface is built to collect port food transportation port food transportation mooring load series. The series is characterized by the fact that it is quite random and complex. In connection with this feature, a prediction method is proposed by which wavelet analysis and BP neural network are combined to build models. Experimental results show that the prediction accuracy of this method is higher than the wavelet neural network method and the traditional neural network method, that it can meet engineering needs and that it can be applied to short-term port food transportation port food transportation mooring load warning systems in harbors.

### ACKNOWLEDGMENT

This study is supported by The National Natural Science Fund (51149001), Innovation of Scientific Research Project of Shanghai Municipal Education Commission (11CXY49).

### REFERENCES

- Dou, H., H. Liu, Z. Wu and X. Yang, 2009. Study of traffic flow predication based on wavelet analysis and autoregressive integrated moving average model. *J. Tongji Univ., Nat. Sci.*, 37(4): 486-489.
- He, G.G., S.F. Ma and Y. Li, 2002. A study on forecasting for time series based on wavelet analysis. *Acta Automat. Sinica*, 28: 1012-1014.
- Liang, J. and T. He, 2011. Water quality prediction based on wavelet analysis and support vector machine. *Comput. Appl. Software*, 28: 83-86.
- Liu, H., H. Tian and Y. Li, 2010. Short-term forecasting optimization algorithm for wind speed from wind farms based on wavelet analysis method and rolling time series method. *J. Cent. South Univ., Sci. Technol.*, 41: 370-375.
- Wang, X., G.H. Bi and J.R. Tang, 2011. Composite forecasting model of sunspot time sequences based on EMD. *Comput. Eng.*, 37: 176-179.
- Wu, F., W.D. Wang, Y.Z. Zhang and Y.F. Zhao, 2010. Magnitude forecasting of earthquake in mainland China based on least squares support vector machine and wavelet analysis. *Earthquake*, 30: 54-59.